https://doi.org/10.5194/gmd-2023-114
Preprint. Discussion started: 10 July 2023

Geoscientific Model Development Discussions

Modeling biochar effects on soil organic carbon on croplands in the MIMICS (MIcrobial-MIneral Carbon Stabilization) model

Mengjie Han[1,2,4], Qing Zhao[1,2,3], Xili Wang[5], Ying-Ping Wang[6], Philippe Ciais[7], Haicheng Zhang[8], Daniel S. Goll[7], Lei Zhu[9], Zhe Zhao[9], Zhixuan Guo[9], Chen Wang[11], Wei Zhuang[12], Fengchang Wu[13], Wei Li[9,10]*

[1]Guangdong Key Laboratory of Integrated Agro-environmental Pollution Control and Management, Institute of Eco-environmental and Soil Sciences, Guangdong Academy of Sciences, Guangzhou 510650, China.
[2]Key Laboratory of Pollution Ecology and Environmental Engineering Institute of Applied Ecology; Institute of Applied Ecology, Chinese Academy of Sciences, Shenyang 110016, China.
[3]National-Regional Joint Engineering Research Center for Soil Pollution Control and Remediation in South China, Guangzhou 510650, China.
[4]University of Chinese Academy of Sciences, Beijing 100049, China.
[5]Economic & Information center, Zhejiang, China.
[6]CSIRO Environment, PMB 1, Aspendale, Victoria 3195 Australia.
[7]Laboratoire des Sciences du Climat et de l'Environnement, LSCE/IPSL, CEA-CNRS-UVSQ, Universit éParis Saclay, 91191, Gif sur Yvette, France.
[8]Sun Yat Sen Univ, Sch Geog & Planning, Guangzhou, Peoples R China.
[9]Department of Earth System Science, Ministry of Education Key Laboratory for Earth System Modeling, Institute for Global Change Studies, Tsinghua University, Beijing 100084, China.
[10]Institute for Carbon Neutrality, Tsinghua University, Beijing 100084, China.
[11]Key Laboratory of Vegetation Restoration and Management of Degraded Ecosystem, South China Botanical Garden, Chinese Academy of Sciences, Guangzhou, China.
[12]Guangdong Institute of Engineering Technology Research Co., Ltd, Guangzhou 510440, China.
[13]State Key Laboratory of Environmental Criteria and Risk Assessment, Chinese Research Academy of Environmental Sciences, Beijing 100012, China.

Correspondence to: Wei Li (wli2019@tsinghua.edu.cn)

Abstract. Biochar application in croplands aims to sequester carbon and improve soil quality, but its impact on soil organic carbon (SOC) dynamics is not represented in most land models used for assessing land-based climate mitigation, therefore we are unable to quantify the effect of biochar applications under different climate conditions or land management. To fill this gap, here we implemented a submodel to represent biochar into a microbial decomposition model named MIMICS (MIcrobial-MIneral Carbon Stabilization). We first calibrate MIMICS with new representations of density-dependent microbial turnover rate, adsorption of available organic carbon on mineral soil particles, and soil moisture effects on decomposition using global field measured cropland SOC at 58 sites. The calibration of MIMICS leads to an increase in explained spatial variation of SOC from 38% in the default version to 47%-52% in the updated model with new representations. We further integrate biochar in MIMICS resolving its effect on microbial decomposition and SOC sorption/desorption and optimize two biochar-related parameters in these processes using 134 paired SOC measurements with and without biochar addition. The MIMICS-biochar version can generally reproduce the short-term (≤ 6 yr) and long-term (8 yr) SOC changes after adding biochar (mean addition rate: 25.6 t ha^{-1}) (R^2 = 0.65 and 0.84) with a low root mean square error

https://doi.org/10.5194/gmd-2023-114
Preprint. Discussion started: 10 July 2023

Geoscientific Model Development Discussions

(RMSE = 3.61 and 3.31 g kg^{-1}). Our study incorporates sorption and soil moisture processes into MIMICS and extends its capacity to simulate biochar decomposition, providing a useful tool to couple with dynamic land models to evaluate the effectiveness of biochar applications on removing CO_2 from the atmosphere.

1. Introduction

Soil organic carbon (SOC) is the largest terrestrial carbon pool, and increasing soil respiration in response to global warming can cause large carbon emissions to the atmosphere (Bond-Lamberty et al., 2018), therefore add further constraint to stabilize future warming under 2 °C. On the other hand, SOC sequestration through improved land management practices has a potential to mitigate climate change by increasing soil carbon accumulation, such as the "4 per mille" project (Minasny et al., 2017).

Due to the limited temporal and spatial coverage of field SOC measurements, soil biogeochemical models have been widely applied to simulate SOC and its response to climate change and human activities (Eglin et al., 2010). Soil carbon models are evolving from first-order kinetics-based models with simple representation of pool sizes and their turnover rates to microbial models with explicit representation of microbial roles in SOC decomposition and stabilization (Manzoni & Porporato, 2009; Sulman et al., 2018). For example, the MIcrobial-MIneral Carbon Stabilization (MIMICS) model is a process-based soil carbon model with explicit representations of nonlinear SOC decomposition dynamics related to microbial physiology, substrate quality, and physical protection of SOC (Wieder et al., 2014; Wieder et al., 2015). This model has been calibrated with global SOC data and can well represent current understanding of SOC decomposition and formation (Wieder et al., 2015), and outperforms conventional first-order decomposition model in simulating spatial variation in SOC stocks in forest ecosystems on continental scale (Zhang et al., 2020). However, the model has not been evaluated for agricultural sites or misses processes that theoretically should influence SOC dynamics, such as density-dependent microbial processes, adsorption of available organic carbon or soil moisture effects.

The microbial interactions at the community level (e.g., competition) play a crucial role in controlling SOC dynamics, but they are not considered in many microbial models (Georgiou et al., 2017), resulting in unrestricted growth of microbial community size with more carbon input (Buchkowski et al., 2017; Wieder et al., 2013). Therefore, these processes have been recently incorporated in a microbial model, leading to improved predictions of SOC at global scales (Zhang et al., 2020). In addition, field experiments show that physicochemical adsorption plays a more important role in controlling DOC fluxes than the biodegradation process (Kalbitz et al., 2005). Although the adsorption mechanism is complex, depending on various factors such as pH, clay content, destruction and formation of soil aggregates (Mayes et al., 2012), some soil carbon models implemented dynamic adsorption and desorption processes controlled by DOC concentration and available mineral surface sites for binding (Wang et al., 2020; Wang et al., 2013). Furthermore, the effect of soil moisture on SOC cannot be ignored

https://doi.org/10.5194/gmd-2023-114
Preprint. Discussion started: 10 July 2023

because it controls microbial activity, substrate availability and further influences soil respiration and nitrogen mineralization (Manzoni et al., 2012; Schimel et al., 2007). A set of empirical functions for the soil moisture effects were proposed for the use in earth system models (ESMs) (Moyano et al., 2013; Camino-Serrano et al., 2018), and a mechanistic moisture function that incorporates physicochemical and biological processes was also developed recently (Yan et al., 2018). For agricultural lands, modeling the SOC decomposition processes is more challenging due to management practices such as tillage and fertilization, which can significantly interrupt carbon cycle and need specific parameterizations.

Biochar application in croplands as a soil amendment can improve the soil quality and increase the crop production (Smith, 2016; Woolf et al., 2010). Meanwhile, because biochar is produced from biomass through pyrolysis processes and is recalcitrant to be decomposed, it is also considered as a promising negative emission technology (NET) for climate mitigation (Fuss et al., 2018; Minx et al., 2018). The carbon dioxide removal (CDR) potential of biochar is estimated to be 0.5~2 $GtCO_2e$ $year^{-1}$ (CO_2 equivalent) (Fuss et al., 2018; Minx et al., 2018). However, biochar application affects SOC mineralization through various processes (Palansooriya et al., 2019; Luo et al., 2017), resulting in positive or negative priming effects (PEs, changes of native SOC mineralization) (Zimmerman et al., 2011). A recent meta-analysis showed that biochar induced negative priming effects on average (-3.8%), but the 95% confidence interval (CI) of -8.1% to 0.8% also covers positive values (Wang et al., 2016a). Biochar may induce positive PEs through stimulating microbial activity by providing additional nutrients for soil microbes (El-Naggar et al., 2019; Li et al., 2019). Positive PEs usually occurred in shorter term (< 2 year), then decreased or changed to being negative over longer term (Luo et al., 2011; Singh & Cowie, 2014; Ding et al., 2017). For example, biochar can reduce SOC available for microbes by enhancing soil aggregate stability through associations between soil minerals and biochar (Zheng et al., 2018). Its porous structure and high surface area with strong adsorption affinity for SOC can thus cause negative PEs (Zimmerman et al., 2011; Lehmann et al., 2021). PEs are also impacted by the properties of biochar (e.g., feedstock type, pyrolysis temperature) and soil climate (e.g., soil moisture) (Ding et al., 2017). Therefore, soil moisture could be closely related to the adsorption capacity of biochar, and needs to be included in the model for predicting PEs of biochar on SOC changes. The biochar decomposition and impacts on native SOC through priming effects are important for the CDR potential of biochar, but these processes are not represented in most land carbon models (Lehmann et al., 2021), precluding the model capacity of fully assessing the effectiveness of large-scale application of biochar as a NET and its environmental impacts.

In this study, we aim to improve the MIMICS model by adding new processes controlling SOC dynamics, especially for cropland and develop a biochar model version that incorporates our current understanding of biochar effects on SOC for future predictions at the regional or global scale. We first added density-dependent microbial turnover rate, adsorption of available organic carbon, and soil moisture effects on microbial decomposition rate into MIMICS which are needed to simulate the

https://doi.org/10.5194/gmd-2023-114
Preprint. Discussion started: 10 July 2023


Geoscientific Model Development Discussions

response of SOC to biochar addition. Parameters in the updated model versions were optimized using 58 field measured cropland SOC concentrations without biochar addition. We then accounted for biochar effects on SOC in MIMICS by calibrating two parameters related to biochar, using 134 paired field SOC measurements in short- and long-term with and without biochar addition.

2. Materials and methods

2.1 Observational data collection

We collected 387 paired field measurements of SOC concentrations (g kg^{-1}) in croplands with or without biochar addition from 58 locations (see the site map in Fig. S1) from published literatures. Soil properties (clay content (Clay), bulk density (BD), soil moisture (SM)), climatic conditions (mean annual temperature (MAT), mean annual precipitation (MAP)), biological variable (net primary productivity (NPP)) and biochar-related characteristics: application rate (Rate_BC), the interval between biochar application and soil sampling (Age_BC), feedstock type (Feedstock_BC), pyrolysis temperature (Temp_BC) were also collected when available. Auxiliary information (e.g., location, and managements, crop cover types) and more detailed information can be found in Han et al. (2021).

Because some sites have multiple biochar addition experiments (e.g., pyrolysis temperature × aging time of biochar), the control SOC concentrations at the same site were averaged, and the SOC concentrations with biochar addition for a given rate (Rate_BC) were also averaged, omitting other characteristics of the BC (like pyrolysis temperature). In total, 134 paired SOC data were used for model calibration (Fig. S1). The depth of soil sampled varies among sites, but is less than 30 cm in general. The biochar application rate has a wide range of 0.9~120 t ha^{-1} with a median value of 20 t ha^{-1} (Fig. S2a). Most biochar addition experiments are short-term with the median Age_BC of 1.2 year (Fig. S2b). The main types of cultivated crop are maize, rice and wheat.

We also used three published global SOC datasets for croplands without biochar addition (Sun et al., 2020; Geisseler et al., 2017; Zhou et al., 2017b) as independent datasets to evaluate the model performance for simulating cropland SOC in general. There are 227 sites in total in these three datasets (Fig. S1).

Soil properties that were not reported in the literature were extracted from gridded datasets using the coordinates of the sites: clay content from Global Soil Dataset for use in Earth System Models (GSDE, Shangguan et al., 2014) and SM from the satellite observations of Soil Moisture Active Passive (SMAP, Entekhabi et al., 2010). Missing soil BD in control treatments were filled according to the relationship between SOC and bulk density based on 4765 cultivated soil data from the 2nd national soil survey (Song et al., 2005), and a decrease of 7.6% (Omondi et al., 2016) from the control soil BD was assumed to

https://doi.org/10.5194/gmd-2023-114
Preprint. Discussion started: 10 July 2023

Geoscientific Model Development Discussions

fill the missing BD values in the biochar addition experiments. The climate variable MAT is extracted from WorldClim (Fick & Hijmans, 2017), and the mean annual aridity index (AI, i.e., precipitation/potential evapotranspiration) used in the soil moisture equation (Eq. 10) was obtained from the Global Aridity Index and Potential Evapotranspiration Database (Zomer et al., 2022). The biological variable (i.e., NPP) is from the MODIS NPP dataset (Zhao & Running, 2010).

2.2 Modifications of the MIMICS model

2.2.1 The default version of MIMICS (MIMICS-def)

The MIMICS model (Wieder et al., 2014; Wieder et al., 2015) includes two microbial functional groups, i.e. copiotrophic (r-strategy) and oligotrophic (k-strategy), and physiological tradeoffs between these two groups. The model explicitly considers the impacts of litter chemical quality by the partitioning of litter input into metabolic and structural litter carbon pools, and stable SOC formation through physical and physicochemical protection of microbial byproducts and leached litter carbon.

There are seven carbon pools in MIMICS including two litter pools, two microbial biomass pools and three SOC pools (Fig. 1, Fig. S3). The litter inputs (LIT) are divided into metabolic (LIT_m) and structural pools (LIT_s) according to the litter quality (f_{met}, i.e., fraction of litter to LIT_m), which is linearly related to the ratio of lignin to nitrogen (lignin:N, Table S1). Microbial growth efficiency (MGE) determines the carbon fluxes from the two litter pools and the available SOC pool (SOC_a) for microbial biomass pools and heterotrophic respiration. The turnover of microbial biomass (τ) depends on the microbes functional types (MIC_r and MIC_k for r- and k-strategy, respectively). Three SOC pools represent the available (SOC_a), physically protected (SOC_p) and chemically recalcitrant SOC (SOC_c). SOC in the protected pools (i.e., SOC_p and SOC_c) are released to the available SOC pool (SOC_a) over time. More detailed description of the model parameters and carbon fluxes can be found in Table S1 and Wieder et al. (2015). The carbon decomposition rate (mg C cm^{-3} hr^{-1}) of the litter and SOC pools is based on a temperature-sensitive Michaelis–Menten kinetics (Allison et al., 2010; Schimel & Weintraub, 2003):

$$\frac{dC_s}{dt} = MIC \times \frac{V_{max} \times C_s}{K_m + C_s} \quad (1)$$

where C_s (mg C cm^{-3}) is the size of a substrate carbon pool (LIT or SOC), and MIC (mg C cm^{-3}) is the size of the microbial carbon pool (MIC_r or MIC_k). V_{max} and K_m are the microbial maximum reaction velocity (mg C (mg MIC)$^{-1}$ hr^{-1}) and the half-saturation constant (mg C cm^{-3}), respectively, which depend on temperature, T, in ℃.

$$V_{max} = e^{V_{slope}T + V_{int}} \times a_v \times V_{mod} \quad (2)$$

$$K_m = e^{K_{slope}T + K_{int}} \times a_k \times K_{mod} \quad (3)$$

where V_{mod} and K_{mod} represent the modifications of V_{max} and K_m based on their dependence on litter quality, microbial

https://doi.org/10.5194/gmd-2023-114
Preprint. Discussion started: 10 July 2023

Geoscientific Model Development Discussions

functional types, and soil texture. a_v and a_k are the tuning coefficients of V_{max} and K_m, respectively. V_{slope} and K_{slope} are the regression coefficients, and V_{int} and K_{int} are the regression intercepts.

The turnover of MIC_r and MIC_k (MIC_τ, mg C cm^{-3} hr^{-1}) at each time step depends on their specific turnover rate (k_{mic}, hr^{-1}), annual total litter input (LIT_{tot}, g C m^{-2} $year^{-1}$) and f_{met}:

$$MIC_\tau = a_\tau \times k_{mic} \times e^{c f_{met}} \times max(min(\sqrt{LIT_{tot}}, 1.2), 0.8) \times MIC \quad (4)$$

where a_τ (=1.0, dimensionless) is the tuning coefficient of k_{mic}. c is the regression coefficient of MIC_r (0.3) and MIC_k (0.1). The carbon inputs from microbial biomass to SOC pools are determined by the microbial biomass turnover.

The carbon transfer from SOC_p to SOC_a (D, mg C cm^{-3} hr^{-1}) represents the deprotection of SOC_p from mineral surfaces or the breakdown of aggregates, calculated as a function of soil clay content (f_{clay}):

$$D = 1.5 \times 10^{-5} \times k_d \times e^{-1.5 f_{clay}} \quad (5)$$

where k_d (=1.0, dimensionless) is a tuning coefficient of the deprotection rate. The parameter values of the default MIMICS version can be found in Table S1.

2.2.2 MIMICS considering density-dependent microbial turnover rate (MIMICS-T)

We incorporated the density-dependent microbial turnover rate into MIMICS following Georgiou et al. (2017) and Zhang et al. (2020). In the MIMICS-T version, we modified Eq. 4 to represent the increased microbial turnover rate with growing microbial biomass density (MIC, mg C cm^{-3}):

$$MIC_\tau = a_\tau \times k_{mic} \times e^{c \times f_{met}} \times max(min(\sqrt{LIT_{tot}}, 1.2), 0.8) \times MIC^\beta \quad (6)$$

where β is the density-dependence exponent.

2.2.3 MIMICS-T with additional representation of sorption (MIMICS-TS)

We then added the adsorption of available SOC into MIMICS following Wang et al. (2013) and Mayes et al. (2012). The MIMICS-TS version includes a new sorption process (the purple arrow from SOC_a to SOC_p in Fig. S3) but keeps the original desorption process (i.e., the yellow arrow from SOC_p to SOC_a in Fig. S3) unchanged. The sorption capacity of SOC_a (Q_{max}) increases with increasing clay content, and the carbon flux of the sorption process is calculated as follows:

$$F_{ads} = K_{ads} \times (1 - \frac{SOC_p}{Q_{max}}) \times SOC_a \quad (7)$$

$$K_{ads} = k_d \times k_{ba} \quad (8)$$

https://doi.org/10.5194/gmd-2023-114
Preprint. Discussion started: 10 July 2023

Geoscientific Model Development Discussions

$$Q_{max} = 10^{(c_1 \times log(\%clay) + c_2)} \quad (9)$$

where F_{ads} is the carbon flux from SOC_a to SOC_p (mg C cm^{-3} hr^{-1}). k_{ba} is the binding affinity, and K_{ads} is the sorption rate of SOC_p which is associated with the deprotection rate (k_d). Q_{max} is the maximum sorption capacity of SOC_p (mg C cm^{-3} soil). c_1 and c_2 are the coefficient for estimating Q_{max} from Mayes et al. (2012).

2.2.4 MIMICS-TS with soil moisture effects (MIMICS-TSM)

Finally, based on MIMICS-TS, we added soil moisture effects on decomposition into MIMICS. We tested two empirical functions for soil moisture used respectively in the Century model (Parton et al., 2000, Eq. 10) and the ORCHIDEE-SOM model (Camino-Serrano et al., 2018, Eq. 11). We also attempted to implement one mechanism-based function that captures the main physicochemical and biological processes of soil moisture in regulating soil respiration from Yan et al. (2018) (Eq. 12). The three functions of soil moisture are illustrated in Fig. S4.

$$f_{m1}(w) = \frac{1}{1 + p_1 \times e^{(p_2 \times w)}} \quad (10)$$

$$f_{m2}(\theta) = max(0.25, min(1, k_1 \times \theta^2 + k_2 \times \theta + k_3) \quad (11)$$

$$f_{m3}\left(\frac{\theta}{\varphi}\right) = \begin{cases} \frac{K_\theta + \theta_{op}}{K_\theta + \theta} \times \left(\frac{\theta}{\theta_{op}}\right)^{(1+an_s)}, & \theta < \theta_{op} \\ \left(\frac{\varphi - \theta}{\varphi - \theta_{op}}\right)^b, & \theta \geq \theta_{op} \end{cases} \quad (12)$$

where f_{mi} (i=1, 2, 3, unitless value in range from 0 to 1) is the response factor to soil moisture. *w* is the soil moisture indicator (AI, mm mm^{-1}). p_1 and p_2 are empirical parameters of soil moisture scalar with p_1 = 30 and p_2= -8.5 (Parton et al., 2000). θ is soil moisture (m^3 m^{-3}). k_1, k_2 and k_3 are soil moist coefficients with 1.1, 2.4 and 0.29, respectively (Camino-Serrano et al., 2018). φ is the soil porosity related to soil bulk density, and θ/φ is the relative water content in soil pores. θ_{op} is an optimum soil moisture content parameter at which the heterotrophic respiration rate peaks. K_θ is moisture constant depending on organic-mineral associations. n_s is saturation exponent depending on soil structure and texture. a and b are SOC-microbial collocation factor and oxygen supply restriction factor, respectively (Yan et al., 2018).

In MIMICS-TSM, the effects of soil moisture on SOC decomposition rate are represented through multiplying the response factor by V_{max} and K_m as follows (Eq. 13, 14).

$$V_{max} = e^{V_{slope} \cdot T + V_{int}} \cdot a_v \cdot V_{mod} \times f_{mi} \quad (13)$$

$$K_m = e^{K_{slope} \cdot T + K_{int}} \cdot a_k \cdot K_{mod} \times f_{mi} \quad (14)$$

The MIMICS models with three soil moisture functions of f_{m1} (Eq. 10), f_{m2} (Eq. 11) and f_{m3} (Eq. 12) are indicated as $MIMICS\text{-}TSM_a$, $MIMICS\text{-}TSM_b$ and $MIMICS\text{-}TSM_c$, respectively. The modifications of all MIMICS versions are

https://doi.org/10.5194/gmd-2023-114
Preprint. Discussion started: 10 July 2023


Geoscientific Model Development Discussions

summarized in Table S2. There are only minor differences in the accuracy of reproducing SOC observation among the three versions (Fig. S11).

Because the MIMICS-TSM$_b$ version with the sorption process and soil moist effects has the best accuracy in reproducing the observations (see **Section 3.1** and Fig. 2), this version was used for further implementation of biochar effects on SOC.

2.2.5 Adjusted parameters for cropland SOC

The metabolic fraction in the total crop litter (f_{met}) is calculated as the mean metabolic fractions in leaf, root and wood, weighted by NPP in the three parts. In order to adapt MIMICS for simulating cropland SOC, we modified the ratio of carbon to nitrogen (C:N) and the ratio of lignin to carbon (lignin:C) in the three parts based on field measurements of main crop types (Abiven et al., 2005, Table S3). The derived ratio of lignin to nitrogen (Lignin:N) is used to determine f_{met} (Table S1). A harvest index (HI) of 0.45 (Hicke & Lobell, 2004) was also applied to remove the harvested part of crop and obtain the litter input to soil (= crop aboveground NPP × (1-HI)).

2.3 Implementing biochar modeling in MIMICS

When applying biochar in croplands, a fraction of biochar (f_{loss} = 2%, Archontoulis et al., 2016) is assumed to be lost during application. Because the sizes of SOC$_p$ and SOC$_c$ pools in MIMICS were not measured directly in the field studies, the 98 % remaining fraction is partitioned into three MIMICS SOC pools by assuming 60% goes to SOC$_p$ based on the measured proportions of added biochar within aggregates (Yoo et al., 2017), 20% goes to SOC$_a$ according to the labile C portion in biochar (Roberts et al., 2010) and 20% goes to SOC$_c$, respectively (Fig. 1). Note that biochar is not treated as a separate carbon pool but assumed to mix with other carbon in existing pool (Fig. 1). In addition to the increase of total SOC, some important processes controlling SOC accumulation and decomposition are affected by biochar addition. We thus modified the parameters related to decomposition and deprotection of SOC (Fig. 1). The associated rationales, equations and parameters are described in the following sections.

https://doi.org/10.5194/gmd-2023-114
Preprint. Discussion started: 10 July 2023

Geoscientific Model Development Discussions

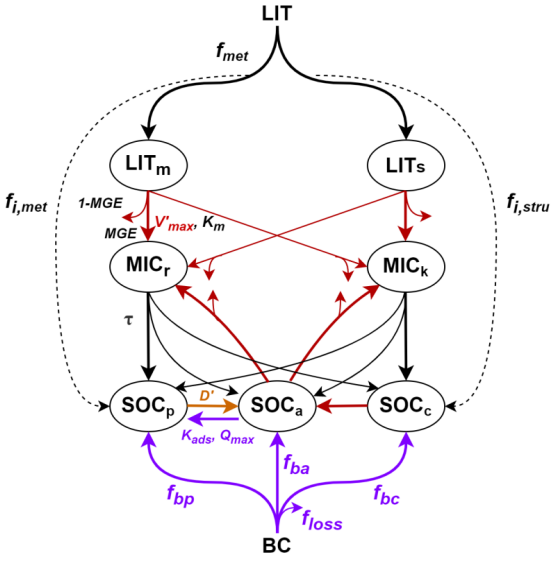

Fig. 1 Framework of the MIMICS model with biochar addition (MIMICS-BC; adapted from Wieder et al. (2015)). The biochar (BC) carbon with a fraction loss (f_{loss}) is partitioned into SOC_p, SOC_a and SOC_c based on f_{bp}, f_{ba} and f_{bc}, respectively. The modified processes with biochar addition are marked with colors, and the purple arrows represent the newly added processes. The deprotection process (orange arrow) is modified through changes in the deprotection rate of SOC_p ($D^{'}$) with biochar addition. The adsorption process (purple arrow) is associated with the adsorption rate (K_{ads}) and the maximum sorption capacity (Q_{max}). The carbon decomposition processes (red arrows) are modified by adjusting the microbial maximum reaction velocity ($V^{'}_{max}$) with biochar addition. The description of other unmodified processes in the default MIMICS model version can be found in Fig. S3.

We assumed that biochar addition decreases the mineralization of native SOC (negative PE) because of its strong adsorption affinity for organic matter (Lehmann et al., 2021). A deprotection coefficient (f_d, ha t^{-1} Rate_BC) was defined as a function of the biochar application rate (Rate_BC) based on Woolf & Lehmann (2012) and Archontoulis et al. (2016), and Eq. 5 was thus modified as:

$$D' = D \times (1 + f_d \times Rate\_BC) \quad (15)$$

where D' (mg C cm^{-3} hr^{-1}) is the new deprotection rate of SOC_p with biochar addition, and a negative value of f_d indicates a negative priming effect.

We also assumed that biochar provides nutrients (e.g., nitrogen and phosphorus) to microbes and stimulate microbial growth and activity, inducing a positive PE to SOC (El-Naggar et al., 2019). We defined a new decomposition rate coefficient (f_v, ha t^{-1} Rate_BC) that is a function of Rate_BC, and included it in MIMICS by modifying Eq. 2:

https://doi.org/10.5194/gmd-2023-114
Preprint. Discussion started: 10 July 2023

Geoscientific Model Development Discussions

$$V'_{max} = V_{max} \times (1 + f_v \times Rate\_BC) \quad (16)$$

where V'_{max} is the new microbial maximum reaction velocity (mg C (mg MIC)$^{-1}$ hr^{-1}) with biochar addition.

2.4 Parameter optimization and model evaluation

All field SOC observations in control plots were assumed at a steady state. SOC pools in MIMICS reach an equilibrium state after about 200 years of model run (Fig. S5). To accelerate this process, we used the analytical spinup method (Xia et al., 2012) to obtain the steady SOC state with the site-level inputs of annual mean crop NPP, MAT, Clay, SM and BD in the parameter optimization. The Shuffled Complex Evolution Algorithm (SCE-UA) has been proven to be a robust method for parameter optimization (Duan et al., 1994; Muttil & Jayawardena, 2008), and the SCE-UA method from the *spotpy* package in python (Houska et al., 2015; https://pypi.org/project/spotpy/) was applied here. Parameters are optimal when the root mean square error (RMSE, Eq. 17) between simulated SOC and observed SOC concentrations is minimized. The Akaike information criterion (AIC, Eq. 18, Akaike, 1974), which considers both model error and the number the model parameters, was also calculated to evaluate different MIMICS versions.

$$RMSE = \sqrt{\frac{\sum_{i=1}^{n}(SOC_{obs,i} - SOC_{sim,i})^2}{n}} \quad (17)$$

$$AIC = n \times ln\left(\frac{\sum_{i=1}^{n}(SOC_{obs,i} - SOC_{sim,i})^2}{n}\right) + 2p \quad (18)$$

Where $SOC_{obs,i}$ and $SOC_{sim,i}$ are the observed and simulated SOC at each i site. n is the number of observations, and p is the number of free model parameters.

The parameters optimized in different MIMICS versions using the entire SOC dataset (i.e., 58 sites) are shown in Table S4. Note that the parameters of soil moisture functions (Eq. 10-12) are directly derived from the original literature (Parton et al., 2000; Camino-Serrano et al., 2018; Yan et al., 2018) and not optimized in MIMICS-TM. We validated the models against our datasets including SOC and auxiliary information (Fig. S1) for the main crop types (maize, rice, and wheat), and the relationships between SOC in these crop types and model input variables (i.e., NPP, MAT, Clay) were analyzed. In addition, all the site SOC data within 0.5 °×0.5 °grid cell were aggregated to match the resolution of model simulations. We also conducted a sensitivity test of MIMICS input variables (i.e., MAT, Clay, NPP, SM and BD) with four perturbation levels of -50%, -25%, 25% and 50% to explore the effects of possible underrepresented processes on the cropland steady SOC.

The cross-validation was also used to evaluate each model version (i.e., MIMICS-def, MIMICS-T, MIMICS-TS, MIMICS-TSM_b) by randomly selecting 80% data for parameter optimization, and the remaining 20% data for model evaluation. The random selection is repeated for 10 times, and the mean R^2, RMSE and AIC were calculated by comparing

https://doi.org/10.5194/gmd-2023-114
Preprint. Discussion started: 10 July 2023


Geoscientific Model Development Discussions

simulated SOC with the observed SOC in test datasets.

For the version of MIMICS with biochar addition, we run parallel simulations with control (without biochar addition) and experimental simulation (with biochar addition) for Age_BC year at hourly time steps, restarted from the previous SOC equilibrium. Not that these simulations for biochar addition are transient runs and thus SOC is not in a steady state. The two model runs are forced by site-level 6-hour temperature data from Climatic Research Unit and Japanese reanalysis data (CRU-JRA, Kobayashi et al., 2015; Harris et al., 2014) and NPP derived from MODIS (Zhao & Running, 2010). The soil-related inputs of Clay, SM and BD are assumed invariant in time and consistent with input data for the steady SOC runs. The absolute SOC changes (ΔSOC, g kg^{-1}, Eq. 19) in the simulated and observed SOC concentrations were compared after BC addition. The RMSE between simulated and observed ΔSOC was minimized using SCE-UA for parameter optimization. AIC and the slopes of regression lines between the simulated and observed SOC changes were analyzed.

$$\Delta SOC = X_t - X_c \quad (19)$$

where X_t and X_c is the observed (or simulated) SOC concentrations with and without biochar addition, respectively.

Three tests were conducted to evaluate the performance of MIMICS-BC on simulating SOC changes after biochar addition using the optimized parameters values in MIMICS-TSM_b (i.e., a_v, a_k, k_d, β, k_{ba}, c_1, c_2; Table 1): 1) without biochar-related parameters; 2) with only one new biochar-related parameter (i.e., the deprotection coefficient, f_d, Eq. 15) optimized (MIMICS-BC_D); 3) with two new biochar-related parameters (i.e., f_d and the decomposition rate coefficient, f_v, Eq. 16) optimized (MIMICS-BC_{DV}). The optimized parameters values in these three tests are shown in Table 1.

Considering the uncertainties in the MIMICS-BC parameters, we conducted a sensitivity test of biochar-related parameters (i.e., f_d, f_v, f_{bp}, f_{ba}) and input variables (i.e., Rate_BC, Age_BC, NPP, Clay, SM) with four perturbation levels of -50%, -25%, 25% and 50% for each site. Because the duration of most biochar addition experiments is short (74.2% data < 3 years), we also extracted data with Age_BC ≥ 3yr (4 yr, 5 yr and 6 yr) and tested the model performance on them separately. Due to lack of field measured data for a longer period, we extended our collected control SOC data to 8 years according to the decomposition curve of biochar in soil fitted by a double first-order exponential decay model (Fig. S6; Wang et al., 2016a). Specifically, the 8-yr SOC data with biochar addition is the sum of field control SOC observations and the residual biochar carbon in soil after 8 years. These extended long-term data were also used for parameter optimization and model evaluation. The relationships between observed ΔSOC and model input variables and the partial correlations between biases (simulated minus observed ΔSOC) from the three tests and model input variables (soil-, climate-, biological-, and biochar-related variables) were also analyzed to detect the possible missing processes.

https://doi.org/10.5194/gmd-2023-114
Preprint. Discussion started: 10 July 2023

Geoscientific Model Development Discussions

Table 1 Parameters for optimization in MIMICS versions.

Datasets	Model versions	Optimized parameters	Prior value	Optimized value	Units
Cropland SOC (58 sites)	MIMICS-TSM$_b$	a_v	10	15.91	-
		a_k	5	13.10	-
		k_d	0.5	1.60	-
		β	1	1.47	-
		k_{ba}	6	2.95	-
		c_1	0.3	0.51	-
		c_2	3	3.86	-
Cropland SOC changes with biochar addition (134 paired data)	MIMICS-TSM$_b$	-	-	-	-
	MIMICS-BC$_D$	f_d	-0.002	-0.0038[a] (-0.0131[b])	ha t^{-1} C
	MIMICS-BC$_{DV}$	f_d	-0.002	-0.0083[a] (-0.0095[b])	ha t^{-1} C
		f_v	0.05	0.008[a] (-0.0097[b])	ha t^{-1} C

Note: a_v and a_k are the tuning coefficients for microbial maximum reaction velocity (Eq. 2) and half-saturation constant (Eq. 3). k_d is the tuning coefficient for deprotection rate of SOC$_p$ (Eq. 5). β is the density-dependent microbial turnover rate (Eq. 6). k_{ba} is binding affinity (Eq. 8), and c_1, c_2 are fitted values for estimating maximum sorption capacity of SOC$_p$ (Eq. 9). f_d and f_v are coefficients for adjusting the deprotection rate of SOC$_p$ (Eq. 15) and microbial decomposition velocity (Eq. 16), respectively when adding biochar. Superscripts a and b are for the optimized parameter values using the short-term and long-term (extended to 8 yr) SOC data, respectively.

3. Results

3.1 Performance of different MIMICS versions for simulating cropland SOC

Among the MIMICS versions without biochar optimized parameters, MIMICS-TSM$_b$ has the highest correlation (R^2=0.52, Fig. 2, Fig. S7) and the lowest RMSE (RMSE=4.41 g kg^{-1}, Fig. 2, Fig. S7) between the observed and simulated cropland SOC concentrations. Compared to MIMICS-def (R^2=0.38, RMSE=4.96 g kg^{-1}, AIC=191.8, Fig. S7), all other MIMICS versions show better performances with a higher R^2 of 0.47~0.52 (Fig. S7). After considering the density-dependent microbial turnover rate, MIMICS-T can better capture the observed spatial variation of SOC (R^2=0.47, RMSE=4.61 g kg^{-1}, AIC=185.3, Fig. 2e, Fig. S7). MIMICS-TS with alternative implementation of SOC$_p$ adsorption explains 51% SOC spatial variation with a smaller RMSE (4.45 g kg^{-1}), but a larger AIC (187.2) (Fig. 2e, Fig. S7). As compared with MIMICS-TS, for the MIMICS-TSM versions that accounts for the effects of soil moisture, R^2 (0.50~0.52) does not show significantly improvement with RMSE and AIC of 4.41~4.53 g kg^{-1} and 186.0~189.2, respectively (Fig. 2; Fig. S7). When using 20% data for the independent model evaluation, MIMICS-TS predicted SOC better with the highest accuracy (R^2=0.38) and the lowest RMSE (4.96 g kg^{-1}), but a higher AIC (52.14) among all different model versions (Table S5).

https://doi.org/10.5194/gmd-2023-114
Preprint. Discussion started: 10 July 2023

Geoscientific Model Development Discussions

We also evaluated the performances of different MIMICS versions using cropland SOC data not used in the calibration (Sun et al., 2020; Geisseler et al., 2017; Zhou et al., 2017b). MIMICS performs comparably well on these SOC datasets. R^2 of different MIMICS versions that were evaluated using the three SOC datasets from Sun et al. (2020), Geisseier et al. (2017) and Zhou et al. (2017b) ranges from 0.38 to 0.80, and R^2 of MIMICS-TSM_b is highest among all MIMICS versions (Fig. S8). The model performance varies among different cover crops (i.e., maize, rice and wheat). R^2 between the simulated SOC concentrations by MIMICS-TSM_b and observations is higher for maize and wheat (0.84 and 0.74, respectively, Fig. S9a, c) but lowest for rice (0.38, Fig. S9b). It is probably because the flooded condition in the paddy field limited SOC decomposition, which is partly supported by the weaker correlation between SOC and NPP for rice (R^2=0.06, Fig. S10d) than that for maize and wheat (R^2=0.77 and 0.54, Fig. S10a, g).

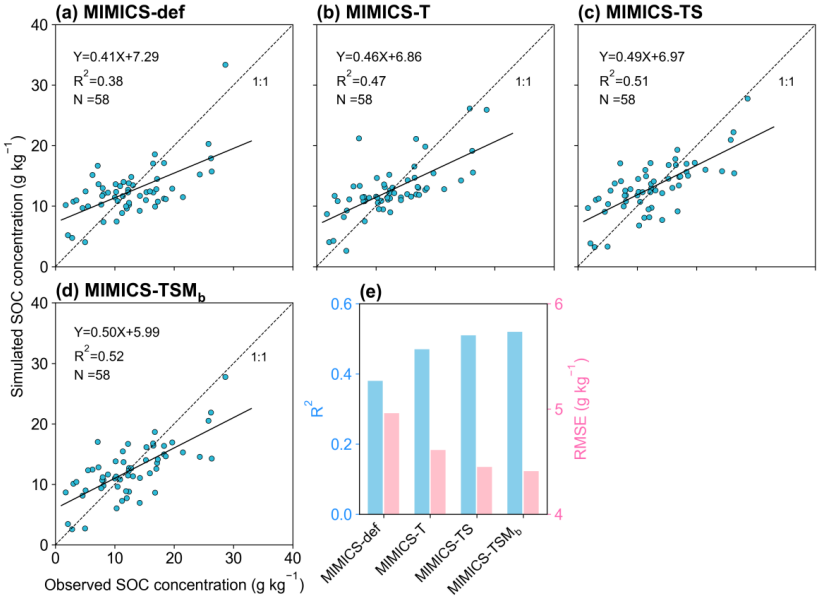

Fig. 2 Relationships between observed and simulated SOC concentrations by various MIMICS versions at cropland sites. MIMICS-def (a) is the default model version with modified parameters related to crop properties (Section 2.2.5); MIMICS-T (b) considers the density-dependent microbial turnover rate; MIMICS-TS (c) also includes the sorption process of SOC_p; MIMICS-TSM_b (d) considers further moisture effects on SOC turnover from the ORCHIDEE-SOM model (Camino-Serrano et al., 2018). (e) R^2 and root mean square error (RMSE) of the four MIMICS versions. Relationships for the other MIMICS versions can be found in Fig. S11.

3.2 Evaluation of the MIMICS-BC model

3.2.1 Model Evaluation

https://doi.org/10.5194/gmd-2023-114
Preprint. Discussion started: 10 July 2023

Geoscientific Model Development Discussions

For short-term SOC changes after biochar addition, the performance of MIMICS-BC_{DV} (R^2 =0.65, RMSE=3.61 g kg^{-1}, Fig. 3d, e) is slightly better than MIMICS-TSM_b (R^2=0.63, RMSE=3.67 g kg^{-1}, Fig. 3) and MIMICS-BC_D (R^2=0.64, RMSE=3.64 g kg^{-1}, Fig. 3d, e), but the AIC (352.57) is higher than that of MIMICS-TSM_b (348.57) and MIMICS-BC_D (350.57) (Fig. 3f). The slope of SOC changes after biochar addition between observations and simulations from MIMICS-BC_D (= 0.77) and MIMICS-BC_{DV} (= 0.76) is also closer to 1 than the MIMICS-TSM_b (= 0.71, Fig. 3a-c). We further evaluated the model performance at sites with a relatively longer biochar addition period of observations (Age_BC ≥ 3 yr). The corresponding R^2 between observed and simulated SOC changes after biochar addition by MIMICS-BC_{DV} (0.09~0.70, Fig. S12c, f, i, l) are lower than that R^2 for all sites (0.65, Fig. 3d), except for sites with Age_BC ≥ 3 yr (0.70, Fig. S12c).

For the long-term (extended to 8 yr based on biochar decomposition curve, Wang et al., 2016a) SOC changes after biochar addition, MIMICS-TSM_b underestimates the exptrapolated observations of SOC change (Fig. 3a). Compared to MIMICS-TSM_b (R^2 =0.89, RMSE=5.62 g kg^{-1}, slope=0.38, AIC=462.76, Fig. 3a, d, e, Fig. 3f), predictions of MIMICS-BC_D and MIMICS-BC_{DV} are more accurate with a smaller RMSE (3.57 g kg^{-1} and 3.31 g kg^{-1}, Fig. 3e), a linear slope closer to 1 (0.87 and 1.00, Fig. 3a-c), a reasonable accuracy of R^2 (0.83 and 0.84, Fig. 3d), but an increase in AIC (464.76 and 466.76, Fig. 3f).

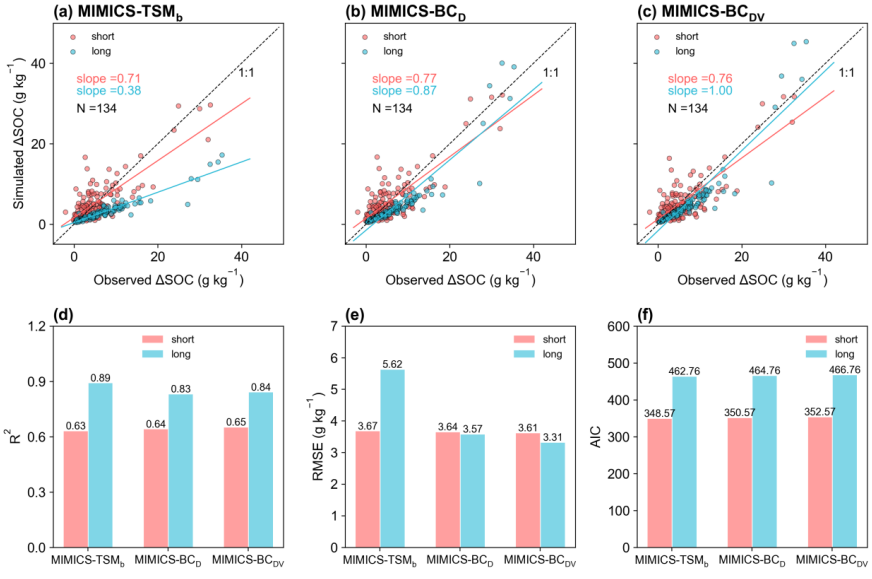

Fig. 3 Relationships of short-term (≤ 6 yr; pink) and long-term (i.e., extended to 8 yr; light blue) SOC changes after biochar addition (ΔSOC) between observations and models. The MIMICS versions are used, including MIMICS-TSM_b (a), MIMICS-BC_D (b) and MIMICS-BC_{DV} (c). Comparisons of R^2 (d), the root mean square error (RMSE, e) and the Akaike information criterion (AIC, f) among the three MIMICS-BC versions are shown separately. MIMICS-TSM_b considers both the sorption process and soil moisture effects but without parameterizations for biochar addition; MIMICS-BC_D includes biochar

https://doi.org/10.5194/gmd-2023-114
Preprint. Discussion started: 10 July 2023

Geoscientific Model Development Discussions

effects on SOC by modifying deprotection rate of SOC_p in the MIMICS-TSM_b (Eq. 15); MIMICS-BC_{DV} considers further biochar effects on SOC by modifying the microbial maximum reaction velocity (Eq. 16).

3.2.2 Error analysis

The biases between the simulated and observed SOC changes with biochar addition in short-term are significantly correlated to Clay and MAT ($p < 0.05$) and decrease only marginally as additional parameters are optimized (Fig. S13). For the long-term SOC changes after biochar addition, the best model version, i.e., MIMICS-BC_{DV}, can explain 84% of the variations of observed long-term SOC changes after biochar addition (Fig. 3c). The biases between long-term observations and simulations by MIMICS-TSM_b are significantly correlated to Rate_BC (r = -0.82), Age_BC (r = -0.22), Clay (r = 0.32) and BD (r = 0.20, Fig. 4), suggesting that the model may underrepresent processes related to those variables. By considering biochar effects on the SOC deprotection (MIMICS-BC_D), the correlations of model biases with Rate_BC, Age_BC, Clay ($p < 0.05$), BD, SM and NPP become weaker (Fig. 4). MIMICS-BC_{DV} incorporating the biochar impacts on microbial decomposition velocity further reduced the correlations between model biases and variables of Rate_BC, Age_BC and BD, but the correlations changed little for Clay and NPP.

Fig. 4 Correlations between the MIMICS-BC biases (i.e., simulated long-term ΔSOC - observed ΔSOC) and input soil- (Clay, BD, SM), climate- (MAT), biological- (NPP) and biochar-related (Rate_BC, Age_BC) variables for MIMICS-TSM_b, MIMICS-BC_D and MIMICS-BC_{DV}. Asterisks indicate significant correlations ($p < 0.05$).

4. Discussion

4.1 Sensitivity tests of MIMICS for simulating cropland SOC

MIMICS versions with adsorption and soil moisture effects perform well in comparison with site-level SOC concentrations on croplands collected in this study and other datasets (Fig. 2; Fig. S8), although the soil moisture effects are not notable. We also tried a test by assuming that soil moisture affects the microbial growth rate through mediating microbial growth (V_{max}) and

https://doi.org/10.5194/gmd-2023-114
Preprint. Discussion started: 10 July 2023

turnover (τ) of MIC_r and MIC_k (Wieder et al., 2019) and thus added the soil moisture factor (i.e., $f(\theta)$ in Eq. 11) on V_{max} and τ. But the model did not predict SOC concentrations more accurately (R^2=0.45, RMSE=4.7 g kg^{-1}, AIC=194, Fig. S14) than the MIMICS-TSM_b version where V_{max} and K_m were affected in (R^2=0.52, RMSE=4.4 g kg^{-1}, AIC=186, Fig. 2d). Annual mean crop NPP, as the input of SOC pools, is also optimized within the range of site-level crop NPP values similarly to other variables to test model performance in MIMICS-TSM_b, but it shows little improvement (R^2=0.45, RMSE=4.7 g kg^{-1}, AIC=196, Fig. S15), compared to MIMICS-TSM_b without NPP optimized (Fig. 2d). Decomposition equations of SOC were constructed based on a wide variety of ecological assumptions, resulting in many forms (Buchkowski et al., 2017). The inverse Michaelis-Menten kinetics of soil carbon decomposition assume that the SOC decomposition rate depends nonlinearly on the enzyme concentration, but linearly on the substrate concentration (Wang et al., 2016b). We also tested MIMICS based on the inverse Michaelis-Menten kinetics in the carbon degradation processes to explore the fundamental mechanisms of SOC decomposition, but the results are similar to the forward Michael-Menten kinetics (Fig. 2; Fig. S16a-d). In addition, we tested MIMICS for different spatial resolutions after aggregating cropland SOC sites within each 0.5 ° × 0.5 °grid cell, and the model also performs well and can reproduce about 50% of the SOC spatial variation (Fig. S16e-h).

SOC dynamics is influenced by many complex factors (e.g., pH, mineral content). In clay- or Fe-rich mineral soils, physically protected SOC might increase due to the large adsorption capacity of dissolved organic carbon onto soil mineral particles (Mayes et al., 2012). Adding the sorption process into MIMICS (MIMICS-TS) indeed improved the model performance (R^2=0.51, Fig. 2c), compared to the MIMICS-T version (R^2=0.47, Fig. 2b). In addition, management (e.g., irrigation, fertilization) are important factors that affect SOC decomposition and accumulation in croplands. The poor performance of MIMICS for rice is probably due to inability of MIMICS to simulate SOC dynamics under anaerobic condition from the irrigation practice (Fig. S9-10). Tillage may disrupt soil aggregates and release physically protected SOC, which is more susceptible to decomposition than that protected by soil aggregates (Six et al., 1999). Juice et al. (2022) modeled tillage effects on SOC loss through transferring protected SOC into unprotected pools, i.e., from SOC_p to SOC_a in this study. Although lacking sufficient tillage information at the sites we studies here, we attempted to include tillage disturbance effects in MIMICS by assuming a fixed 30% increase of deprotection rate of SOC_p according to Juice et al. (2022) (i.e., D ×(1+30%), Eq. 5), but R^2 between observations and simulations (0.46~0.51, Fig. S16i-l) is similar to that from the version without tillage (R^2 = 0.47~0.52, Fig. 2).

In addition, cropland management disturbs soils frequently, and the assumed equilibrium state of SOC may not be realistic, which also partly explains the mismatch between simulated and observed SOC. We thus added sensitivity tests by perturbing the input variables (MAT, Clay, NPP, SM and BD) to evaluate the steady SOC changes and the possible impacts of non-steady states on the results. The size of SOC pool is positively correlated with NPP and Clay, but negatively correlated with MAT and

https://doi.org/10.5194/gmd-2023-114
Preprint. Discussion started: 10 July 2023

BD. The responses of steady SOC to the perturbation of BD, MAT and NPP are relatively large (Fig. S17), indicating that processes related to these variables have a great effect on the steady SOC. The soil BD was found to be affected by tillage practices (Osunbitan et al., 2005), and crop NPP may vary due to crop rotation, fallow or fertilization. Therefore, agricultural management practices, such as fertilization and crop rotation, need to be incorporated in soil carbon models in future to reduce the uncertainty of simulating cropland SOC dynamics (Campbell et al., 2007; Congreves et al., 2015).

4.2 Sensitivity tests and uncertainty for MIMICS-BC

The MIMICS-BC versions have a good performance in reproducing the observed short-term SOC changes with biochar addition (R^2 = 0.63~0.65, Fig. 3). It is probably due to the high correlation between Rate_BC and ΔSOC (r = 0.74, Fig. S13), indicating that the biochar application rate dominates changes in SOC concentrations over a short period. For the long-term changes (extended to 8 yr), MIMICS-BC versions show a greater improvement than the MIMICS-TSM_b version (Fig. 3). Biochar can absorb SOC due to its large specific surface area, high porosity and further promotion of soil macro-aggregates formation (Han et al., 2020; Huang et al., 2018). Consistently, the optimized deprotection coefficient (f_d = -0.0038 and -0.0131 for short- and long-term, Table 1) in MIMICS-BC_D is negative, indicating the carbon deprotection from SOC_p to SOC_a is reduced with biochar addition, and the biochar effect on SOC sorption/desorption over long term is stronger than that in short term. Incorporating the biochar impacts on microbial decomposition velocity in the MIMICS-BC_{DV} further improved model with biochar addition in long term (decomposition rate coefficient (f_v) = -0.0097, Table 1). MIMICS-BC_{DV} further reduced the correlations between model-observation biases and input variables, but the correlation with Clay is still significant ($p < 0.05$, Fig. 4), implying that some processes related to the variable are not well represented in the model. The responses of ΔSOC to parameter perturbations show that f_v and f_d affect ΔSOC changes with biochar addition in opposite directions, and ΔSOC is more sensitive to the partition coefficient from biochar carbon to SOC_p (f_{bp}) than f_d, f_v and the partition coefficient from biochar carbon to SOC_a (f_{ba}) (Fig. 5). Among the input variables, ΔSOC is more sensitive to Rate_BC than Age_BC.

Biochar stability, which could affect priming effects, varies with biochar feedstock types and pyrolysis temperature (Yang et al., 2021). Using wood and straw as biochar feedstock, 0.3% and 0.8% of biochar carbon is lost at a pyrolysis temperature of 800 °C (wood) and 350 °C (straw), respectively (Hamer et al., 2004). 2% of biochar carbon was assumed to distribute into active/metabolic pool in the EPIC model (The Environmental Policy Integrated Climate, Lychuk et al., 2014), and thus we tested the MIMICS-BC model with the partition coefficient from biochar carbon to SOC_a (f_{ba}) =2%, and the model shows a lower R^2 (0.6, Fig. S18) than that f_{ba} = 20% in short-term (0.65, Fig. 3). We further optimized the partition coefficient from biochar carbon to SOC_p (f_{bp}) and f_{ba} based on MIMICS-BC_{DV} to test the parameter uncertainties. The optimized version (MIMICS-BC_{DV*}) shows a better performance (R^2=0.67, RMSE=3.6 g kg^{-1}, AIC=350, Fig. S19) than MIMICS-$BC_{DV,}$ and the optimized f_{bp}, f_{ba} and the partition coefficient from biochar carbon to SOC_c (f_{bc}) are 59.6%, 29.1% and 11.3%, respectively.

https://doi.org/10.5194/gmd-2023-114
Preprint. Discussion started: 10 July 2023

Geoscientific Model Development Discussions

Correlations of MIMICS-BC$_{DV*}$ model errors with Clay are reduced, but the correlations with Rate_BC and BD are increased (Fig. S13).

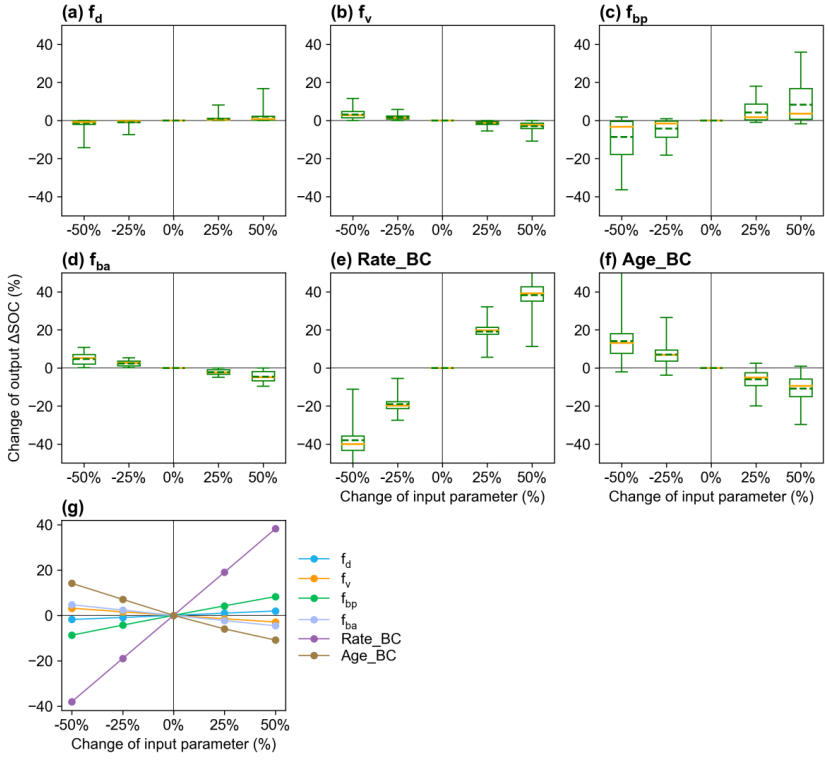

Fig. 5 Sensitivity analysis of MIMICS-BC model parameters of (a) f_d (deprotection coefficient, Eq. 15), (b) f_v (decomposition rate coefficient, Eq. 16), (c) f_{bp} (partition coefficient from biochar carbon to SOC$_p$, Fig. 1), (d) f_{ba} (partition coefficient from biochar carbon to SOC$_a$, Fig. 1), and the biochar-related input variables, (e) Rate_BC and (f) Age_BC. The yellow line and green dotted line in boxplots are median and mean values of the changes in model output (i.e., change of ΔSOC, Eq. 19). The mean values of change of output ΔSOC in all sites are shown in (g).

The effects of biochar on SOC are controlled by various factors, such as soil physicochemical and biological properties (e.g., clay, pH, microbial activity), biochar properties (e.g., feedstock, pyrolysis temperature) and incubation conditions (e.g., periods, cover crop types) (Ding et al., 2017; Han et al., 2020). Some of these effects are not explicitly considered in the MIMICS biochar version. Microbial carbon use efficiency (CUE) determines the relation proportions of microbial carbon uptake between growth and respiration (Zhou et al., 2017a), and increased CUE and reduced turnover time (1/τ) of microbial biomass were found with biochar addition, although the changes depend on the soil texture (Pei et al., 2021). We conducted additional sensitivity tests with assumed perturbation levels in these parameters (MGE and τ) and input variables (NPP, Clay and SM) in the simulations with biochar addition. MGE and τ are very important parameters to the model outputs, while the

https://doi.org/10.5194/gmd-2023-114
Preprint. Discussion started: 10 July 2023

impacts of NPP, Clay and SM are relatively small (Fig. S20). Therefore, processes and parameters related to MGE and τ need to be accounted for in future with more evidence.

Biochar addition may also change the composition of microbial community, and a previous study reported increased copiotrophic bacteria with a higher growth rate and decreased oligotrophic bacteria in acid soils with biochar addition (Sheng & Zhu, 2018). This is related to the competition between r- and k-strategy microbes in MIMICS. In the MIMICS-BC version, we assumed that biochar, with a longer turnover time (about 1000 yr, Schmidt et al., 2002) than SOC, are evenly mixed with SOC and are treated as a homogenous pool without an explicit vertical profile, which may also bring uncertainties. In addition, due to lack of long-term biochar addition experiments, the extended long-term SOC concentrations with biochar addition is calculated as the sum of SOC in the control site without biochar addition and the remaining biochar carbon based on the biochar degradation curve (Fig. S6; Wang et al., 2016a). Although they are not direct observations and may induce uncertainty, the long-term model validation is important to assess the model ability of simulating the SOC stability with biochar addition. Long-term and comprehensive field measurements of SOC and other soil and microbe properties after biochar addition are therefore urgently needed to understand the underlying mechanisms of biochar impacts on SOC changes, all of which will help improve the model performance.

5. Conclusion

In this study, we developed several updated MIMICS versions with new processes (e.g., adsorption and soil moisture) and attempted to incorporate biochar into MIMICS to simulate the effects of biochar on SOC dynamics. We further validated MIMICS against field measurements on global croplands without and with biochar addition. However, management practices such as tillage, fertilization and irrigation on croplands are intensive, raising challenges in representing these processes in the soil carbon models due to lack of spatially explicit input data and poor understanding of the mechanisms. Therefore, more long-term field experiments for biochar addition will help better represent biochar processes in the soil carbon model and evaluate the model performance. Biochar is believed to have a large CDR potential, and its application on soils would affect the soil carbon and nutrient cycles. These impacts need to be incorporated ESMs to accurately simulate the mitigation potential of biochar under future climate change.

Code availability. The codes of this model version are available at https://doi.org/10.5281/zenodo.8112967 (Han et al., 2023).

Author contributions. Mengjie Han collected the site measurements data for model evaluation, performed the simulations and optimized the model code, and prepared the manuscript. Qing Zhao and Wei Li conceived the study and designed the experiments. Wei Li, Ying-Ping Wang, Philippe Ciais, Haicheng Zhang, Daniel S. Goll, Chen Wang and Wei Zhuang guided

https://doi.org/10.5194/gmd-2023-114
Preprint. Discussion started: 10 July 2023

and improved the manuscript in technology, logic and detail. Lei Zhu, Zhe Zhao and Zhixuan Guo assisted with the technical aspects in data acquisition and analysis. Xili Wang and Fengchang Wu reviewed and revised the manuscript.

Competing interests. The authors declare that they have no conflict of interest.

Acknowledgements. This study was funded by the National Natural Science Foundation of China (grant number: 42192574, 42022056, 42175169) and Tsinghua University Initiative Scientific Research Program (grant number: 20223080041).

References

Abiven, S., Recous, S., Reyes, V., & Oliver, R.: Mineralisation of C and N from root, stem and leaf residues in soil and role of their biochemical quality, *Biology and Fertility of Soils, 42*, 119-128, doi:10.1007/s00374-005-0006-0, 2005.

Akaike, H.: A new look at the statistical model identification, *IEEE transactions on automatic control, 19*, 716-723. 1974.

Allison, S. D., Wallenstein, M. D., & Bradford, M. A.: Soil-carbon response to warming dependent on microbial physiology, *Nature Geoscience, 3*, 336-340, doi:10.1038/ngeo846, 2010.

Archontoulis, S. V., Huber, I., Miguez, F. E., Thorburn, P. J., Rogovska, N., & Laird, D. A.: A model for mechanistic and system assessments of biochar effects on soils and crops and trade-offs, *GCB Bioenergy, 8*, 1028-1045, doi:10.1111/gcbb.12314, 2016.

Bond-Lamberty, B., Bailey, V. L., Chen, M., Gough, C. M., & Vargas, R.: Globally rising soil heterotrophic respiration over recent decades, *Nature, 560*, 80-83, doi:10.1038/s41586-018-0358-x, 2018.

Buchkowski, R. W., Bradford, M. A., Grandy, A. S., Schmitz, O. J., & Wieder, W. R.: Applying population and community ecology theory to advance understanding of belowground biogeochemistry, *Ecol Lett, 20*, 231-245, doi:10.1111/ele.12712, 2017.

Camino-Serrano, M., Guenet, B., Luyssaert, S., Ciais, P., Bastrikov, V., De Vos, B., Gielen, B., Gleixner, G., Jornet-Puig, A., Kaiser, K., Kothawala, D., Lauerwald, R., Peñuelas, J., Schrumpf, M., Vicca, S., Vuichard, N., Walmsley, D., & Janssens, I. A.: ORCHIDEE-SOM: modeling soil organic carbon (SOC) and dissolved organic carbon (DOC) dynamics along vertical soil profiles in Europe, *Geoscientific Model Development, 11*, 937-957, doi:10.5194/gmd-11-937-2018, 2018.

Campbell, C. A., VandenBygaart, A. J., Zentner, R. P., McConkey, B. G., Smith, W., Lemke, R., Grant, B., & Jefferson, P. G.: Quantifying carbon sequestration in a minimum tillage crop rotation study in semiarid southwestern Saskatchewan, *Canadian Journal of Soil Science, 87*, 235-250, doi:10.4141/s06-018, 2007.

Congreves, K. A., Grant, B. B., Campbell, C. A., Smith, W. N., VandenBygaart, A. J., Kröbel, R., Lemke, R. L., & Desjardins, R. L.: Measuring and Modeling the Long-Term Impact of Crop Management on Soil Carbon Sequestration in the Semiarid Canadian Prairies, *Agronomy Journal, 107*, 1141-1154, doi:10.2134/agronj15.0009, 2015.

Ding, F., Van Zwieten, L., Zhang, W., Weng, Z., Shi, S., Wang, J., & Meng, J.: A meta-analysis and critical evaluation of influencing factors on soil carbon priming following biochar amendment, *Journal of Soils and Sediments, 18*, 1507-1517, doi:10.1007/s11368-017-1899-6, 2017.

Duan, Q. Y., Sorooshian, S., & Gupta, V. K.: Optimal use of the SCE-UA global optimization method for calibrating watershed models, *Journal of Hydrology, 158*, 265-284, doi:10.1016/0022-1694(94)90057-4, 1994.

Eglin, T., Ciais, P., Piao, S. L., Barre, P., Bellassen, V., Cadule, P., Chenu, C., Gasser, T., Koven, C., Reichstein, M., & Smith, P.: Historical and future perspectives of global soil carbon response to climate and land-use changes, *Tellus B: Chemical and Physical Meteorology, 62*, 700-718, doi:10.1111/j.1600-0889.2010.00499.x, 2010.

El-Naggar, A., El-Naggar, A. H., Shaheen, S. M., Sarkar, B., Chang, S. X., Tsang, D. C. W., Rinklebe, J., & Ok, Y. S.: Biochar composition-dependent impacts on soil nutrient release, carbon mineralization, and potential environmental risk: A review, *J Environ Manage, 241*, 458-467, doi:10.1016/j.jenvman.2019.02.044, 2019.

Entekhabi, D., Njoku, E. G., O'Neill, P. E., Kellogg, K. H., Crow, W. T., Edelstein, W. N., Entin, J. K., Goodman, S. D.,

https://doi.org/10.5194/gmd-2023-114
Preprint. Discussion started: 10 July 2023

Jackson, T. J., Johnson, J., Kimball, J., Piepmeier, J. R., Koster, R. D., Martin, N., McDonald, K. C., Moghaddam, M., Moran, S., Reichle, R., Shi, J. C., Spencer, M. W., Thurman, S. W., Tsang, L., & Van Zyl, J.: The Soil Moisture Active Passive (SMAP) Mission, *Proceedings of the IEEE, 98*, 704-716, doi:10.1109/jproc.2010.2043918, 2010.

Fick, S. E., & Hijmans, R. J.: WorldClim 2: new 1-km spatial resolution climate surfaces for global land areas, *International Journal of Climatology, 37*, 4302-4315, doi:10.1002/joc.5086, 2017.

Fuss, S., Lamb, W. F., Callaghan, M. W., Hilaire, J., Creutzig, F., Amann, T., Beringer, T., de Oliveira Garcia, W., Hartmann, J., Khanna, T., Luderer, G., Nemet, G. F., Rogelj, J., Smith, P., Vicente, J. L. V., Wilcox, J., del Mar Zamora Dominguez, M., & Minx, J. C.: Negative emissions—Part 2: Costs, potentials and side effects, *Environmental Research Letters, 13*, doi:10.1088/1748-9326/aabf9f, 2018.

Geisseler, D., Linquist, B. A., & Lazicki, P. A.: Effect of fertilization on soil microorganisms in paddy rice systems – A meta-analysis, *Soil Biology and Biochemistry, 115*, 452-460, doi:10.1016/j.soilbio.2017.09.018, 2017.

Georgiou, K., Abramoff, R. Z., Harte, J., Riley, W. J., & Torn, M. S.: Microbial community-level regulation explains soil carbon responses to long-term litter manipulations, *Nat Commun, 8*, 1223, doi:10.1038/s41467-017-01116-z, 2017.

Hamer, U., Marschner, B., Brodowski, S., & Amelung, W.: Interactive priming of black carbon and glucose mineralisation, *Organic Geochemistry, 35*, 823-830. 2004.

Han, L., Sun, K., Yang, Y., Xia, X., Li, F., Yang, Z., & Xing, B.: Biochar's stability and effect on the content, composition and turnover of soil organic carbon, *Geoderma, 364*, doi:10.1016/j.geoderma.2020.114184, 2020.

Han, M., Zhao, Q., Li, W., Ciais, P., Wang, Y. P., Goll, D. S., Zhu, L., Zhao, Z., Wang, J., Wei, Y., & Wu, F.: Global soil organic carbon changes and economic revenues with biochar application, *GCB Bioenergy, 14*, 364-377, doi:10.1111/gcbb.12915, 2021.

Harris, I., Jones, P. D., Osborn, T. J., & Lister, D. H.: Updated high-resolution grids of monthly climatic observations - the CRU TS3.10 Dataset, *International Journal of Climatology, 34*, 623-642, doi:10.1002/joc.3711, 2014.

Hicke, J. A., & Lobell, D. B.: Spatiotemporal patterns of cropland area and net primary production in the central United States estimated from USDA agricultural information, *Geophysical Research Letters, 31*. 2004.

Houska, T., Kraft, P., Chamorro-Chavez, A., & Breuer, L.: SPOTting Model Parameters Using a Ready-Made Python Package, *PLoS One, 10*, e0145180, doi:10.1371/journal.pone.0145180, 2015.

Huang, R., Tian, D., Liu, J., Lv, S., He, X., & Gao, M.: Responses of soil carbon pool and soil aggregates associated organic carbon to straw and straw-derived biochar addition in a dryland cropping mesocosm system, *Agriculture, Ecosystems & Environment, 265*, 576-586, doi:10.1016/j.agee.2018.07.013, 2018.

Juice, S. M., Walter, C. A., Allen, K. E., Berardi, D. M., Hudiburg, T. W., Sulman, B. N., & Brzostek, E. R.: A new bioenergy model that simulates the impacts of plant-microbial interactions, soil carbon protection, and mechanistic tillage on soil carbon cycling, *GCB Bioenergy, 14*, 346-363, doi:10.1111/gcbb.12914, 2022.

Kalbitz, K., Schwesig, D., Rethemeyer, J., & Matzner, E.: Stabilization of dissolved organic matter by sorption to the mineral soil, *Soil Biology and Biochemistry, 37*, 1319-1331, doi:10.1016/j.soilbio.2004.11.028, 2005.

Kobayashi, S., Ota, Y., Harada, Y., Ebita, A., Moriya, M., Onoda, H., Onogi, K., Kamahori, H., Kobayashi, C., Endo, H., Miyaoka, K., & Takahashi, K.: The JRA-55 Reanalysis: General Specifications and Basic Characteristics, *Journal of the Meteorological Society of Japan. Ser. II, 93*, 5-48, doi:10.2151/jmsj.2015-001, 2015.

Lehmann, J., Cowie, A., Masiello, C. A., Kammann, C., Woolf, D., Amonette, J. E., Cayuela, M. L., Camps-Arbestain, M., & Whitman, T.: Biochar in climate change mitigation, *Nature Geoscience, 14*, 883-892, doi:10.1038/s41561-021-00852-8, 2021.

Li, Z., Song, Z., Singh, B. P., & Wang, H.: The impact of crop residue biochars on silicon and nutrient cycles in croplands, *Sci Total Environ, 659*, 673-680, doi:10.1016/j.scitotenv.2018.12.381, 2019.

Luo, Y., Durenkamp, M., De Nobili, M., Lin, Q., & Brookes, P. C.: Short term soil priming effects and the mineralisation of biochar following its incorporation to soils of different pH, *Soil Biology and Biochemistry, 43*, 2304-2314, doi:10.1016/j.soilbio.2011.07.020, 2011.

Luo, Y., Zang, H., Yu, Z., Chen, Z., Gunina, A., Kuzyakov, Y., Xu, J., Zhang, K., & Brookes, P. C.: Priming effects in biochar enriched soils using a three-source-partitioning approach: 14C labelling and 13C natural abundance, *Soil Biology*

https://doi.org/10.5194/gmd-2023-114
Preprint. Discussion started: 10 July 2023

and Biochemistry, 106, 28-35. 2017.

Lychuk, T. E., Izaurralde, R. C., Hill, R. L., McGill, W. B., & Williams, J. R.: Biochar as a global change adaptation: predicting biochar impacts on crop productivity and soil quality for a tropical soil with the Environmental Policy Integrated Climate (EPIC) model, *Mitigation and Adaptation Strategies for Global Change, 20*, 1437-1458, doi:10.1007/s11027-014-9554-7, 2014.

Manzoni, S., & Porporato, A.: Soil carbon and nitrogen mineralization: Theory and models across scales, *Soil Biology and Biochemistry, 41*, 1355-1379, doi:10.1016/j.soilbio.2009.02.031, 2009.

Manzoni, S., Schimel, J. P., & Porporato, A.: Responses of soil microbial communities to water stress: results from a meta-analysis, *Ecology, 93*, 930-938, doi:10.1890/11-0026.1, 2012.

Mayes, M. A., Heal, K. R., Brandt, C. C., Phillips, J. R., & Jardine, P. M.: Relation between Soil Order and Sorption of Dissolved Organic Carbon in Temperate Subsoils, *Soil Science Society of America Journal, 76*, 1027-1037, doi:10.2136/sssaj2011.0340, 2012.

Minasny, B., Malone, B. P., McBratney, A. B., Angers, D. A., Arrouays, D., Chambers, A., Chaplot, V., Chen, Z.-S., Cheng, K., Das, B. S., Field, D. J., Gimona, A., Hedley, C. B., Hong, S. Y., Mandal, B., Marchant, B. P., Martin, M., McConkey, B. G., Mulder, V. L., O'Rourke, S., Richer-de-Forges, A. C., Odeh, I., Padarian, J., Paustian, K., Pan, G., Poggio, L., Savin, I., Stolbovoy, V., Stockmann, U., Sulaeman, Y., Tsui, C.-C., Vågen, T.-G., van Wesemael, B., & Winowiecki, L.: Soil carbon 4 per mille, *Geoderma, 292*, 59-86, doi:10.1016/j.geoderma.2017.01.002, 2017.

Minx, J. C., Lamb, W. F., Callaghan, M. W., Fuss, S., Hilaire, J., Creutzig, F., Amann, T., Beringer, T., de Oliveira Garcia, W., Hartmann, J., Khanna, T., Lenzi, D., Luderer, G., Nemet, G. F., Rogelj, J., Smith, P., Vicente Vicente, J. L., Wilcox, J., & del Mar Zamora Dominguez, M.: Negative emissions—Part 1: Research landscape and synthesis, *Environmental Research Letters, 13*, doi:10.1088/1748-9326/aabf9b, 2018.

Moyano, F. E., Manzoni, S., & Chenu, C.: Responses of soil heterotrophic respiration to moisture availability: An exploration of processes and models, *Soil Biology and Biochemistry, 59*, 72-85, doi:10.1016/j.soilbio.2013.01.002, 2013.

Muttil, N., & Jayawardena, A. W.: Shuffled Complex Evolution model calibrating algorithm: enhancing its robustness and efficiency, *Hydrological Processes, 22*, 4628-4638, doi:10.1002/hyp.7082, 2008.

Omondi, M. O., Xia, X., Nahayo, A., Liu, X., Korai, P. K., & Pan, G.: Quantification of biochar effects on soil hydrological properties using meta-analysis of literature data, *Geoderma, 274*, 28-34, doi:10.1016/j.geoderma.2016.03.029, 2016.

Osunbitan, J., Oyedele, D., & Adekalu, K.: Tillage effects on bulk density, hydraulic conductivity and strength of a loamy sand soil in southwestern Nigeria, *Soil and Tillage Research, 82*, 57-64. 2005.

Palansooriya, K. N., Wong, J. T. F., Hashimoto, Y., Huang, L., Rinklebe, J., Chang, S. X., Bolan, N., Wang, H., & Ok, Y. S.: Response of microbial communities to biochar-amended soils: a critical review, *Biochar, 1*, 3-22, doi:10.1007/s42773-019-00009-2, 2019.

Parton, W. J., Morgan, J. A., Kelly, R. H., & Ojima, D.: Modeling soil C responses to environmental change in grassland systems[M] The potential of US grazing lands to sequester carbon and mitigate the greenhouse effect. 2000.

Pei, J., Li, J., Mia, S., Singh, B., Wu, J., & Dijkstra, F. A.: Biochar aging increased microbial carbon use efficiency but decreased biomass turnover time, *Geoderma, 382*, doi:10.1016/j.geoderma.2020.114710, 2021.

Roberts, K. G., Gloy, B. A., Joseph, S., Scott, N. R., & Lehmann, J.: Life Cycle Assessment of Biochar Systems: Estimating the Energetic, Economic, and Climate Change Potential, *Environmental Science & Technology, 44*, 827-833, doi:10.1021/es902266r, 2010.

Schimel, J., Balser, T. C., & Wallenstein, M.: Microbial stress-response physiology and its implications for ecosystem function, *Ecology, 88*, 1386-1394, doi:10.1890/06-0219, 2007.

Schimel, J. P., & Weintraub, M. N.: The implications of exoenzyme activity on microbial carbon and nitrogen limitation in soil: a theoretical model, *Soil Biology and Biochemistry, 35*, 549-563. 2003.

Schmidt, M. W., Skjemstad, J. O., & Jäger, C.: Carbon isotope geochemistry and nanomorphology of soil black carbon: Black chernozemic soils in central Europe originate from ancient biomass burning, *Global Biogeochemical Cycles*,

https://doi.org/10.5194/gmd-2023-114
Preprint. Discussion started: 10 July 2023

16, 70-71-70-78. 2002.

Shangguan, W., Dai, Y., Duan, Q., Liu, B., & Yuan, H.: A global soil data set for earth system modeling, *Journal of Advances in Modeling Earth Systems, 6*, 249-263, doi:10.1002/2013ms000293, 2014.

Sheng, Y., & Zhu, L.: Biochar alters microbial community and carbon sequestration potential across different soil pH, *Sci Total Environ, 622-623*, 1391-1399, doi:10.1016/j.scitotenv.2017.11.337, 2018.

Singh, B. P., & Cowie, A. L.: Long-term influence of biochar on native organic carbon mineralisation in a low-carbon clayey soil, *Scientific reports, 4*, 1-9. 2014.

Six, J., Elliott, E., & Paustian, K.: Aggregate and soil organic matter dynamics under conventional and no-tillage systems, *Soil Science Society of America Journal, 63*, 1350-1358. 1999.

Smith, P.: Soil carbon sequestration and biochar as negative emission technologies, *Glob Chang Biol, 22*, 1315-1324, doi:10.1111/gcb.13178, 2016.

Song, G., Li, L., Pan, G., & Zhang, Q.: Topsoil organic carbon storage of China and its loss by cultivation, *Biogeochemistry, 74*, 47-62, doi:10.1007/s10533-004-2222-3, 2005.

Sulman, B. N., Moore, J. A. M., Abramoff, R., Averill, C., Kivlin, S., Georgiou, K., Sridhar, B., Hartman, M. D., Wang, G., Wieder, W. R., Bradford, M. A., Luo, Y., Mayes, M. A., Morrison, E., Riley, W. J., Salazar, A., Schimel, J. P., Tang, J., & Classen, A. T.: Multiple models and experiments underscore large uncertainty in soil carbon dynamics, *Biogeochemistry, 141*, 109-123, doi:10.1007/s10533-018-0509-z, 2018.

Sun, W., Canadell, J. G., Yu, L., Yu, L., Zhang, W., Smith, P., Fischer, T., & Huang, Y.: Climate drives global soil carbon sequestration and crop yield changes under conservation agriculture, *Glob Chang Biol, 26*, 3325-3335, doi:10.1111/gcb.15001, 2020.

Wang, G., Huang, W., Zhou, G., Mayes, M. A., & Zhou, J.: Modeling the processes of soil moisture in regulating microbial and carbon-nitrogen cycling, *Journal of Hydrology, 585*, doi:10.1016/j.jhydrol.2020.124777, 2020.

Wang, G., Post, W. M., & Mayes, M. A.: Development of microbial-enzyme-mediated decomposition model parameters through steady-state and dynamic analyses, *Ecological Applications, 23*, 255-272, doi:10.1890/12-0681.1, 2013.

Wang, J., Xiong, Z., & Kuzyakov, Y.: Biochar stability in soil: meta-analysis of decomposition and priming effects, *Global Change Biology Bioenergy, 8*, 512-523, doi:10.1111/gcbb.12266, 2016a.

Wang, Y. P., Jiang, J., Chen-Charpentier, B., Agusto, F. B., Hastings, A., Hoffman, F., Rasmussen, M., Smith, M. J., Todd-Brown, K., Wang, Y., Xu, X., & Luo, Y. Q.: Responses of two nonlinear microbial models to warming and increased carbon input, *Biogeosciences, 13*, 887-902, doi:10.5194/bg-13-887-2016, 2016b.

Wieder, W. R., Bonan, G. B., & Allison, S. D.: Global soil carbon projections are improved by modelling microbial processes, *Nature Climate Change, 3*, 909-912. 2013.

Wieder, W. R., Grandy, A. S., Kallenbach, C. M., & Bonan, G. B.: Integrating microbial physiology and physio-chemical principles in soils with the MIcrobial-MIneral Carbon Stabilization (MIMICS) model, *Biogeosciences, 11*, 3899-3917, doi:10.5194/bg-11-3899-2014, 2014.

Wieder, W. R., Grandy, A. S., Kallenbach, C. M., Taylor, P. G., & Bonan, G. B.: Representing life in the Earth system with soil microbial functional traits in the MIMICS model, *Geoscientific Model Development, 8*, 1789-1808, doi:10.5194/gmd-8-1789-2015, 2015.

Wieder, W. R., Sulman, B. N., Hartman, M. D., Koven, C. D., & Bradford, M. A.: Arctic soil governs whether climate change drives global losses or gains in soil carbon, *Geophysical Research Letters, 46*, 14486-14495. 2019.

Woolf, D., Amonette, J. E., Street-Perrott, F. A., Lehmann, J., & Joseph, S.: Sustainable biochar to mitigate global climate change, *Nat Commun, 1*, 56, doi:10.1038/ncomms1053, 2010.

Woolf, D., & Lehmann, J.: Modelling the long-term response to positive and negative priming of soil organic carbon by black carbon, *Biogeochemistry, 111*, 83-95, doi:10.1007/s10533-012-9764-6, 2012.

Xia, J. Y., Luo, Y. Q., Wang, Y. P., Weng, E. S., & Hararuk, O.: A semi-analytical solution to accelerate spin-up of a coupled carbon and nitrogen land model to steady state, *Geoscientific Model Development, 5*, 1259-1271, doi:10.5194/gmd-5-1259-2012, 2012.

Yan, Z., Bond-Lamberty, B., Todd-Brown, K. E., Bailey, V. L., Li, S., Liu, C., & Liu, C.: A moisture function of soil

https://doi.org/10.5194/gmd-2023-114
Preprint. Discussion started: 10 July 2023

heterotrophic respiration that incorporates microscale processes, *Nat Commun*, *9*, 2562, doi:10.1038/s41467-018-04971-6, 2018.

Yang, Q., Zhou, H., Bartocci, P., Fantozzi, F., Masek, O., Agblevor, F. A., Wei, Z., Yang, H., Chen, H., Lu, X., Chen, G., Zheng, C., Nielsen, C. P., & McElroy, M. B.: Prospective contributions of biomass pyrolysis to China's 2050 carbon reduction and renewable energy goals, *Nat Commun*, *12*, 1698, doi:10.1038/s41467-021-21868-z, 2021.

Yoo, G., Kim, H., & Choi, J. Y.: Soil Aggregate Dynamics Influenced by Biochar Addition using the13C Natural Abundance Method, *Soil Science Society of America Journal*, *81*, 612-621, doi:10.2136/sssaj2016.09.0313, 2017.

Zhang, H., Goll, D. S., Wang, Y. P., Ciais, P., Wieder, W. R., Abramoff, R., Huang, Y., Guenet, B., Prescher, A. K., Viscarra Rossel, R. A., Barre, P., Chenu, C., Zhou, G., & Tang, X.: Microbial dynamics and soil physicochemical properties explain large-scale variations in soil organic carbon, *Glob Chang Biol*, doi:10.1111/gcb.14994, 2020.

Zhao, M., & Running, S. W.: Drought-induced reduction in global terrestrial net primary production from 2000 through 2009, *Science*, *329*, 940-943, doi:10.1126/science.1192666, 2010.

Zheng, H., Wang, X., Luo, X., Wang, Z., & Xing, B.: Biochar-induced negative carbon mineralization priming effects in a coastal wetland soil: Roles of soil aggregation and microbial modulation, *Sci Total Environ*, *610-611*, 951-960, doi:10.1016/j.scitotenv.2017.08.166, 2018.

Zhou, H., Zhang, D., Wang, P., Liu, X., Cheng, K., Li, L., Zheng, J., Zhang, X., Zheng, J., Crowley, D., van Zwieten, L., & Pan, G.: Changes in microbial biomass and the metabolic quotient with biochar addition to agricultural soils: A Meta-analysis, *Agriculture Ecosystems & Environment*, *239*, 80-89, doi:10.1016/j.agee.2017.01.006, 2017a.

Zhou, M., Zhu, B., Wang, S., Zhu, X., Vereecken, H., & Bruggemann, N.: Stimulation of N_2O emission by manure application to agricultural soils may largely offset carbon benefits: a global meta-analysis, *Glob Chang Biol*, *23*, 4068-4083, doi:10.1111/gcb.13648, 2017b.

Zimmerman, A. R., Gao, B., & Ahn, M.-Y.: Positive and negative carbon mineralization priming effects among a variety of biochar-amended soils, *Soil Biology and Biochemistry*, *43*, 1169-1179, doi:10.1016/j.soilbio.2011.02.005, 2011.

Zomer, R. J., Xu, J., & Trabucco, A.: Version 3 of the Global Aridity Index and Potential Evapotranspiration Database, *Sci Data*, *9*, 409, doi:10.1038/s41597-022-01493-1, 2022.